ARCHIVES
OF THERMODYNAMICS

Unsteady flow of a couple stress fluid due to sudden withdrawal of pressure gradient in a parallel plate channel

Donga Anjali[a], Naresh Reddimalla[a], Josyula Venkata Ramana Murthy[a*]

[a]Department of Mathematics, National Institute of Technology Warangal, Telangana 506004, India
*Corresponding author email: jvr@nitw.ac.in

Abstract

The investigation of the couple stress fluid flow behaviour between two parallel plates under sudden stoppage of the pressure gradient is considered. Initially, a flow of couple stress fluid is developed between the two parallel plates under a constant pressure gradient. Suddenly, the applied pressure gradient is stopped, and the resulting unsteady flow is studied. This type of flow is known as run-up flow in the literature. Now the flow is expected to come to rest in a long time. Usually, these types of problems are solved by using the Laplace transform technique. There are difficulties in obtaining the inverse Laplace transform; hence, many researchers adopt numerical inversions of Laplace transforms. In this paper, the problem is solved by using the separation of variables method. This method is easier than the transform method. The velocity field is analytically obtained by applying the usual no-slip condition and hyper-stick conditions on the plates, and hence the volumetric flow rate is derived at subsequent times. The steady state solution before the withdrawal of the pressure gradient is matched with the initial condition on time. The rest time, i.e. the time taken by the fluid to come to rest after the pressure gradient is withdrawn is calculated. The graphs for the velocity field at different times and different couple stress parameters are drawn. In the special case when a couple stress parameter approaches infinity, couple stress fluid becomes a viscous fluid. Our results are in good agreement with this special case.

1. Introduction

A couple stress fluid displays distinctive behaviour, shaped by internal rotational effects resulting from the interaction of forces and moments within the material. In fluid mechanics, these properties influence how the fluid responds to external forces, impacting factors like flow characteristics, stress distribution, and deformation. In unsteady flow, the dynamic behaviour of a couple stress fluid is characterized by the interaction of rota-

tional forces within the material, impacting fluid flow patterns and responses, particularly in the presence of changes in external forces. The couple stress fluid based on pure kinematic behaviour was proposed mathematically by Stokes in 1966 [1]. The couple stress fluid shows the rotational effects and sustention of couple stresses which were not observed for Newtonian fluids. The properties of the couple stress fluids when they flow past a sphere and spheroid have been studied [2]. A method was developed for free convection in magnetohydrodynamics (MHD)

Anjali D., Reddimalla N., Ramana Murthy J.V.

Nomenclature

G – nondimensional pressure gradient
h – half of the distance between the plates, m
P – pressure, Pa
p – nondimensional pressure
Q – volumetric flow rate, m^3/s
S – couple stress parameter
t – nondimensional time
T – time, s
U – velocity in Y- direction, m/s
u – nondimensional velocity
u_s – steady state velocity, m/s
u_t – transient state velocity, m/s

Greek symbols
η – coefficient of couple stress viscosity, N s
λ – separation constant
μ – coefficient of viscosity, Pa s
ρ – density of the fluid, kg/m^3

Abbreviations and Acronyms
HAM – homotopy analysis method
LHS – left hand side
MHD – magnetohydrodynamic
RHS – right hand side

flows using Laplace transforms, which was applied to a thermal shock problem [3]. The authors compared the results between the analytic and numerical solutions by applying the HAM technique and shooting method on the axisymmetric flow of an electrically conducting viscous fluid in the presence of a magnetic field over a non-linear stretching sheet [4]. The authors focused on the exact solution for an MHD boundary layer problem for momentum and heat transfer in Jeffrey fluid flow over a non-isothermal stretching sheet in the presence of dissipative energy, thermal radiation, and internal heat source [5]. The effects of Soret and Dufour on velocity, temperature, and concentration were discussed in the three-dimensional MHD flow of Oldroyd-B fluid [6]. Heat transfer and effects of various embedding parameters on the flow were discussed on three-dimensional flow couple stress fluid with convective boundary conditions by employing the HAM technique [7]. The authors investigated non-Newtonian fluid flows due to the sudden application of pressure gradient. In their study, the velocity field is obtained by Laplace transforms and by separation of variables [8,9]. The effects of directional permeability on the Couette flow of immiscible Newtonian fluids are explored in an anisotropic medium [10]. The authors examined the flow of electrically conducting immiscible Newtonian fluids with variable viscosity through an inclined channel under the influence of a magnetic field [11]. The fourth-order accuracy boundary value problem is applied to get the numerical solution by considering slip conditions on the magnetic effect on radiative inclined magneto-hydrodynamic mixed convection hybrid nanofluid flow through an inclined shrinking permeable plate [12]. The author used the HAM technique to examine the couple stress fluid flow between two curved plates with the porous medium [13]. The entropy production in a couple stress fluid flow regions is observed to be smaller than that of the micro-polar fluid flow region [14]. They examined the flow of electrically conducting immiscible Newtonian fluids with variable viscosity through an inclined channel in the presence of a magnetic field [15]. The authors investigated the characteristics of entropy production, temperature-dependent thermal conductivity, variable viscosity, and a couple stress parameters on non-immiscible fluids in an inclined porous channel [16].

A special type of flow named "run-up flows" for the case of viscoelastic fluids was introduced by Kazakia and Rivlin [17].

Later Rivlin used Laplace transforms theoretically and extensively to investigate the flows formed in run-up flows [18–20]. Almost in the same period, a similar problem of step jump velocities in shear flows was studied by Narain and Joseph [21]. Researchers explored the run-up flows of couple stress fluids and micro-polar fluids through the application of Laplace transforms [22,23]. Additionally, the study delved into the run-up flows of Maxwell fluids, employing Laplace transforms as well [24]. Subsequent investigations were extended to explore run-up flows, considering Hall effects on the flow of Rivlin-Erickson fluids [25]. Another aspect of interest involved the examination of run-up flows of conducting liquid within an annulus [26]. Notably, recent research focused on magneto-hydrodynamic (MHD) fluid run-up flows, employing Laplace transforms for analysis [27]. Many authors solved the problems with run-up and similar flows using numerical inversion of Laplace transform techniques [28,29]. As an extension of [22], the present work investigates the unsteady flow of a couple stress fluid between two parallel plates using the separation of variables technique. The advantage of this method is that it is easy to obtain solutions and can avoid the difficulty in inverting Laplace transforms.

2. Statement of the problem and mathematical formulation

Examining the fully developed steady flow of incompressible couple stress fluid between two parallel plates under a constant pressure gradient, we investigate the scenario where the pressure gradient is suddenly stopped. This leads to the study of the subsequent transient flow, focusing on the extended period required for the fluid to rest. We derive the duration for the fluid to reach a state of rest and estimate the volumetric flow rate during this process.

The linear momentum equation for a couple stress fluid [1] is given by:

$$\rho \frac{\partial U}{\partial T} = -\frac{\partial P}{\partial X} + \mu \frac{\partial^2 U}{\partial Y^2} - \eta \frac{\partial^4 U}{\partial Y^4}, \qquad (1)$$

where p is the pressure, ρ is the density, T is time, μ and η are coefficients of viscosity and couple stress viscosity, respectively.

We introduce the following non-dimensional scheme:

$$X = hx, \quad Y = hy, \quad T = \frac{\rho h^2 t}{\mu}, \quad U = \frac{\mu u}{\rho h},$$

$$P = \frac{\mu^2}{\rho h^2} p, \quad S^2 = \frac{h^2 \mu}{\eta}. \tag{2}$$

The quantities on LHS are physical quantities and non-dimensional quantities are on RHS.

Substituting Eq. (2) in Eq. (1), we get the following non-dimensional equation for velocity u:

$$\rho \frac{\partial u}{\partial t} = -\frac{\partial p}{\partial x} + \frac{\partial^2 u}{\partial y^2} - \frac{1}{S^2} \frac{\partial^4 u}{\partial y^4}. \tag{3}$$

Equation (3) can be solved under the following conditions (Fig. 1):

1. No slip condition $u = 0$ at $y = \pm 1$.
2. Hyper stick condition (angular velocity is zero $\nabla \times \bar{q} = 0$, where $\bar{q}$ is fluid velocity) gives: $\frac{\partial u}{\partial y} = 0$ at $y = \pm 1$. In general, when the surface is under rotation, we take type A condition, or no couple stresses condition on the surface. When the surface is not under rotation, we take type B condition or no angular velocity or hyper-stick condition on the surface.

3. $\frac{\partial p}{\partial x} = \begin{cases} -G & \text{for} \quad t < 0, \\ 0 & \text{for} \quad t \geq 0. \end{cases}$
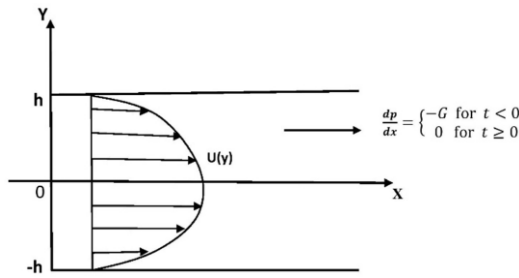

Fig. 1. Graphical representation of the problem.

3. Solution procedure

We assume the solution for Eq. (3) as

$$u = \begin{cases} u_s(y) & \text{for} \quad t < 0, \\ u_t(y,t) & \text{for} \quad t \geq 0, \end{cases} \tag{4}$$

where u_s is steady state fully developed flow under constant pressure gradient G and u_t is transient or unsteady state solution such that:

$$0 = G + \frac{\partial^2 u_s}{\partial y^2} - \frac{1}{S^2} \frac{\partial^4 u_s}{\partial y^4}, \tag{5}$$

and

$$\frac{\partial u_t}{\partial t} = \frac{\partial^2 u_t}{\partial y^2} - \frac{1}{S^2} \frac{\partial^4 u_t}{\partial y^4}. \tag{6}$$

Equations (5) and (6) are subjected to the following conditions:

$$u_s(\pm 1) = 0, \; u_t(\pm 1, t) = 0, \; \frac{\partial u_s}{\partial y}(\pm 1) = 0, \; \frac{\partial u_t}{\partial y}(\pm 1, t) = 0, \tag{7}$$

and $u_t(y, 0) = u_s$ and $u_t(y, t) = 0$ as $t \to \infty$.

Equation (5) is an ordinary differential equation and is re-written as:

$$u_s^{\prime v} - S^2 u_s^{\prime\prime} = S^2 G. \tag{8}$$

The solution of Eq. (8) under conditions for u_s in Eq. (7) is:

$$u_s(y) = \frac{G}{2}(1 - y^2) + \frac{G}{S \sinh S}(\cosh Sy - \cosh S). \tag{9}$$

We assume the solution of Eq. (6) in the form

$$u_t(y, t) = E(y)F(t). \tag{10}$$

Substituting Eq. (10) in Eq. (6) and rearranging we get

$$\frac{F'}{F} = \frac{E'' - \frac{1}{S^2}E^{\prime v}}{E} = -\lambda^2, \tag{11}$$

where F' is derivative with respect to t and E' is derivative with respect to y, the separation constant is taken as negative to satisfy the condition at $t = \infty$.

This gives $F' + \lambda^2 F = 0$ and $E^{\prime v} - S^2 E'' - \lambda^2 S^2 E = 0$ with the auxiliary equation $m^4 - S^2 m^2 - \lambda^2 S^2 = 0$, i.e.

$$m^2 = \frac{S^2 \pm \sqrt{S^2 + 4S^2 \lambda^2}}{2} = \frac{S^2}{2}\left(1 \pm \sqrt{1 + \frac{4\lambda^2}{S^2}}\right),$$

$$m_{1,2} = \pm \frac{S}{\sqrt{2}}\sqrt{1 + \sqrt{1 + \frac{4\lambda^2}{S^2}}},$$

and

$$m_{3,4} = \pm \frac{S}{\sqrt{2}}\sqrt{1 - \sqrt{1 + \frac{4\lambda^2}{S^2}}},$$

are the roots of the auxiliary equation.

The solution for u_t is given by:

$$u_t(y, t) = \sum_\lambda e^{-\lambda^2 t} (A_\lambda \cosh m_1 y + B_\lambda \sinh m_1 y +$$

$$+ C_\lambda \cos m_3 y + D_\lambda \sin m_3 y). \tag{12}$$

Constants in Eq. (12) are found from the conditions in Eq. (7):

$u_t(1, t) = 0 \Rightarrow A\cosh m_1 + B\sinh m_1 + C\cos m_3 + D\sin m_3 = 0$

$u_t(-1, t) = 0 \Rightarrow A\cosh m_1 - B\sinh m_1 + C\cos m_3 - D\sin m_3 = 0$

which implies:

$$B\sinh m_1 + D\sin m_3 = 0,$$

and

$$A\cosh m_1 + C\cos m_3 = 0.$$

Again $\frac{\partial u_t}{\partial y}(1, t) = 0$ gives:

$m_1 A\sinh m_1 + m_1 B\cosh m_1 + m_3 C\sin m_3 + m_3 D\cos m_3 = 0$

and $\frac{\partial u_t}{\partial y}(-1, t) = 0$ gives:

$-m_1 A\sinh m_1 + m_1 B\cosh m_1 + m_3 C\sin m_3 + m_3 D\cos m_3 = 0$

which implies that $\quad m_1 A\sinh m_1 - m_3 C\sin m_3 = 0$

and $\quad\quad\quad m_1 B\cosh m_1 + m_3 D\cos m_3 = 0.$

Then, from equations of B and D, we get:

$$B = -D\frac{\sin m_3}{\sinh m_1} = -D\frac{m_3\cos m_3}{m_1\cosh m_1}, \qquad (13)$$

and from equations of A and C, we get:

$$A = -C\frac{\cos m_3}{\cosh m_1} = C\frac{m_3\sin m_3}{m_1\sinh m_1}. \qquad (14)$$

Substituting (13) and (14) in Eq. (12), we get:

$$u_t(y,t) = \sum e^{-\lambda^2 t} A\left\{\cosh m_1 y - \frac{\cosh m_1}{\cos m_3}\cos m_3 y\right\} +$$
$$+ \sum e^{-\lambda^2 t} B\left\{\sinh m_1 y - \frac{\sinh m_1}{\sin m_3}\sin m_3 y\right\}. \qquad (15)$$

Rearranging Eq. (14) we get:

$$z = m_1\tanh m_1 + m_3\tan m_3 = 0. \qquad (16)$$

The zeroes of Eq. (16) will give the values of the separation constant λ.

The initial condition at $t=0$, $u_t(y,t)=u_s(y)$, yields $B=0$ (since u_t is an even function, the odd function terms will vanish). Hence at $t=0$, we have:

$$\frac{G}{2}(1-y^2) + \frac{G\coth S}{S}\left(\frac{\cosh Sy}{\cosh S}-1\right) = \sum A_n\left(\frac{\cosh m_1 y}{\cosh m_1} - \frac{\cos m_3 y}{\cos m_3}\right). \qquad (17)$$

From Eq. (11) at a fixed value of S, for a range of λ from 0 to 100, we find m_1 and m_3 values. With these values of m_1 and m_3, we obtain z from Eq. (16). Thus, we can plot for z for the values of λ as shown in Fig. 2.

From this graph, the roots for λ are obtained, and then m_1 and m_3 corresponding to these roots λ are found from Eq. (11).
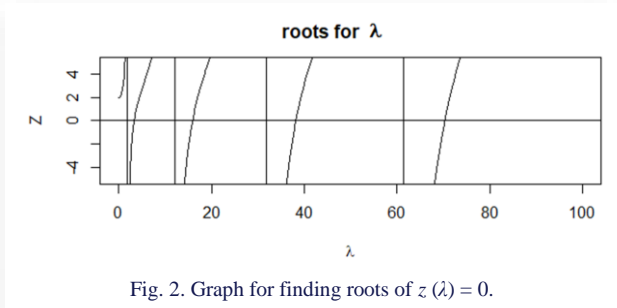

Fig. 2. Graph for finding roots of $z(\lambda)=0$.

The first five roots for λ and the corresponding values for m_1 and m_3 are shown in Table 1.

Table 1. The first five values of separation constant λ.

n	λ_n	$z(\lambda_n)$	m_1	m_3
1	3.297	0.000399	2.981	2.2115
2	15.909	−0.00088	5.8207	5.4663
3	38.193	−0.00074	8.8551	8.6262
4	70.305	0.00042	11.9425	11.7739
5	112.271	0.0008	15.0516	14.9181

To obtain A_n, we solve n equations from Eq. (17) by evaluating Eq. (17) at n equally spaced points y_i, or alternately multiply Eq. (17) by $\left(\frac{\cosh m_1 y}{\cosh m_1} - \frac{\cos m_3 y}{\cos m_3}\right)$ and integrate w.r.t. y between the limits −1 to 1. We get n equations in A_n, and A_n is

obtained by solving this system. The values of A_n by collocation method are given in Table 2.

Table 2. The values of A_n.

Coefficients	A_1	A_2	A_3	A_4	A_5
Values	0.6821	0.0137	0.00156	0.00035	0.000013

We observe that the collocation method gives a very accurate solution. Then finally, we get:

$$u_t = u_t(y,t\geq 0) = \sum_{n=1}^{5} e^{-\lambda_n^2 t} A_n\left(\frac{\cosh m_1 y}{\cosh m_1} - \frac{\cos m_3 y}{\cos m_3}\right), \qquad (18)$$

and the volumetric flow rate Q at any time t is given by:

$$Q = 2\sum_{n=1}^{\infty} e^{-\lambda_n^2 t} A_n\left(\frac{\tanh m_1}{m_1} - \frac{\tan m_3}{m_3}\right). \qquad (19)$$

4. Results and discussion

The unsteady flow of a couple stress fluid between two parallel plates due to the sudden withdrawal of an applied constant pressure gradient is studied. The expressions for the velocity for the transient state and volumetric flow rate are derived and shown in Eqs. (18) and (19), respectively. The velocity profiles for u_t versus distance y at different times t at fixed couple stress parameters ($S = 2$) are shown in Fig. 3a for $G = 5$ and Fig. 3b for $G = 10$, respectively. From Fig. 3, we notice that for 0.5 units of time, u_t becomes almost zero, i.e. the flow comes to rest by 0.5 units of non-dimensional time. And we observe that as G increases, the velocity increases. Initially, velocity starts from higher values and becomes zero by about 0.5 units of times at $S = 2$. This is because when the pressure gradient increases, the applied force on the flow increases, increasing velocity.
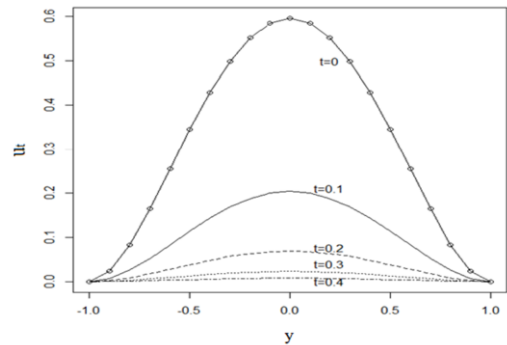
a)
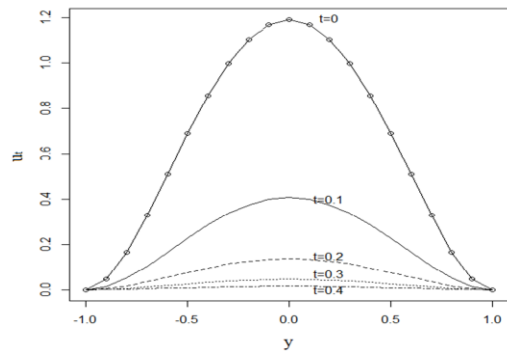
b)

Fig. 3. Velocity profiles (u_t) for $S = 2$ at pressure gradient $G = 5$ (a) and pressure gradient $G = 10$ (b), for various time values.

182

The velocity profiles u_t at fixed pressure gradient ($G = 10$) for various values of couple stress parameter (S) are depicted in Fig. 4a for $t = 0.1$ and Fig. 4b for $t = 0.6$, respectively. From Fig. 4, one can observe that, as the couple stress parameter increases, the velocity values also increase, which is in good agreement with [22]. As S increases, couple stresses decrease, leading to a reduction in the energy required for particle rotation and subsequently causing an increase in velocity. As S increases, the fluid approaches viscous fluid as a limiting case. Consequently, we can infer that viscous fluids consistently exhibit higher velocities compared to fluids with couple stresses at any given time.

a)

b)

Fig. 4. Velocity profiles (u_t) at $G = 10$, $t = 0.1$ (a) and $G = 10$, $t = 0.6$ (b), for various values of couple stress parameter (S).

Figure 5 depicts the relationship between the pressure gradient and rest time for different values of the couple stress parameter (S). It is observed that with an increase in the couple stress parameter, the rest time also increases. Moreover, as the pressure gradient rises, the rest time experiences a gradual increase. This is because, as observed in Fig. 4, as S increases, couple stresses decrease and hence the energy spent for generating couples and rotation decreases; hence, fluid takes more time to rest.

Figure 6 illustrates the time versus volumetric flow rate for various couple stress parameter values. Notably, the flow rate rapidly decreases to zero as time progresses. Additionally, an increase in the couple stress parameter (S) corresponds to an increase in the volumetric flow rate. Consequently, we deduce that

in the limiting case of a couple stress fluid, viscous fluids exhibit higher volumetric flow rates and velocities compared to corresponding couple stress fluids. This result correlates with the observations in Fig. 3 and Fig. 4. As S increases, velocity increases and hence, the volumetric flow rate also increases.
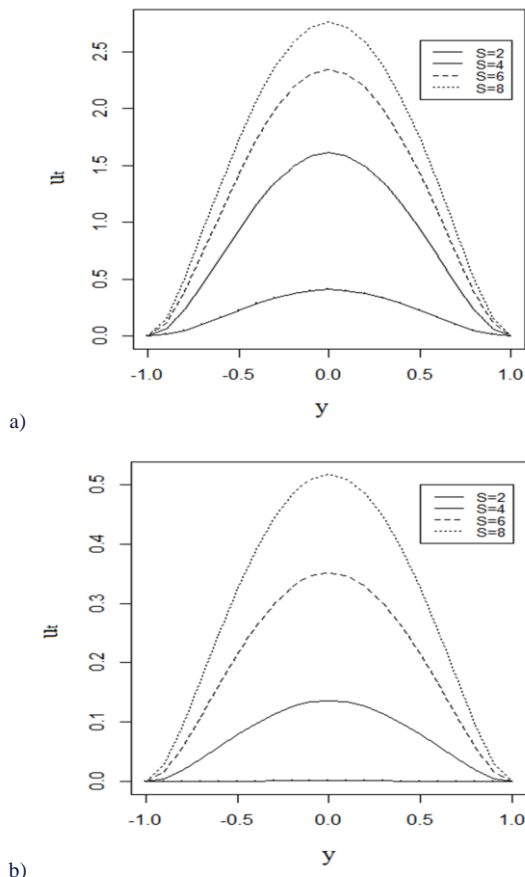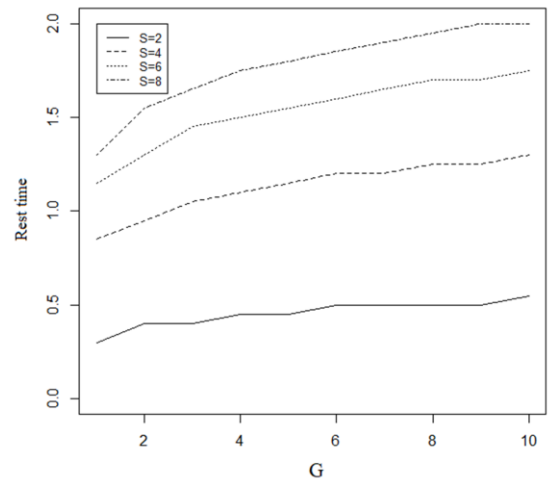

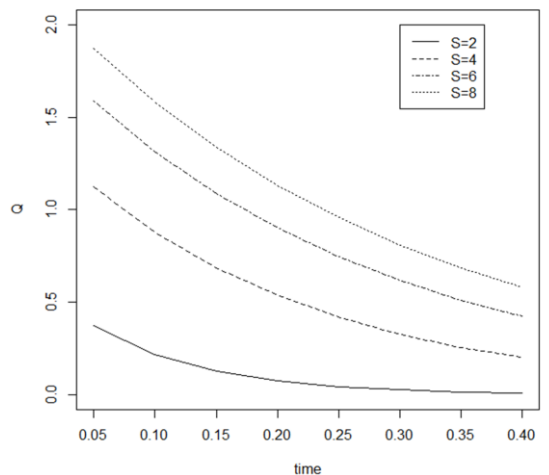Fig. 5. Pressure gradient vs. rest time at different values of S.

Fig. 6. Time vs. volumetric flow rate (Q) for varying values of S.

5. Conclusions

This paper examines the unsteady flow of a couple stress fluid between two parallel plates following the sudden removal of a pressure gradient. The initial state involves both upper and lower plates being stationary, and flow initiation occurs through a constant pressure gradient. The study focuses on the flow patterns resulting from the sudden withdrawal of the pressure gradient, observing that the flow eventually stops after a certain duration. It is observed that:

- The velocity for viscous fluids is more than for the couple stress fluids at any given time.
- Viscous fluids take longer to rest than couple stress fluids.
- A rise in pressure gradient slowly increases the rest time of the fluid.

- The volumetric flow rate at any given time for viscous fluids is more than for the couple stress fluids.

References

[1] Stokes, V.K. (1984). Couple stresses in fluids. In *Theories of Fluids with Microstructure: An Introduction* (pp. 34−80). Springer, Berlin, Heidelberg.

[2] Rao, S.L., & Iyengar, T.K.V. (1985). *Analytical and computational studies in couple stress fluid flows:* UGC Research project C-8-4/82 SR III.

[3] Ezzat, M.A. (2001). Free convection effects on perfectly conducting fluid. *International Journal of Engineering Science*, 39(7), 799−819. doi: 10.1016/S0020-7225(00)00059-8

[4] Ali, R., Nazar, M., Bilal, M., & Salem, A. (2016). Analytic and numerical solutions for axisymmetric flow with partial slip. *Engineering with Computers*, 32, 149−154. doi: 10.1007/s00366-015-0405-2

[5] Ahmed, J., Khan, Z.H., Malik, M.Y., Hussain, A., & Gayathri, D. (2015). A note on convective heat transfer of an MHD Jeffrey fluid over a stretching sheet. *AIP Advances*, 5(11), 117117. doi: 10.1063/1.4935571

[6] Farooq, A., Ali, R., & Benim, A.C. (2018). Soret and Dufour effects on three-dimensional Oldroyd-B fluid. *Physica A: Statistical Mechanics and Its Applications*, 503, 345−354. doi: 10.1016/j.physa.2018.02.204

[7] Ali, R., Hussain, M.Y., Jamil, M., & Suleman, M. (2020). Computational approach on three-dimensional flow of couple-stress fluid with convective boundary conditions. *Physica A: Statistical Mechanics and Its Applications*, 553, 124056. doi: 10.1016/j.physa.2019.124056

[8] Erdogan, M.E., & Imrak, C.E. (2005). On unsteady unidirectional flows of a second grade fluid. *International Journal of Non-Linear Mechanics*, 40(10), 1238−1251. doi: 10.1016/j.ijnonlinmec.2005.05.004

[9] Erdoğan, M.E., & Imrak, C.E. (2007). On some unsteady flows of a non-Newtonian fluid. *Applied Mathematical Modelling*, 31(2), 170−180. doi: 10.1016/j.apm.2005.08.019

[10] Jaiswal, S., & Yadav, P.K. (2023). Physics of generalized Couette flow of immiscible fluids in anisotropic porous medium. *International Journal of Modern Physics B*, 2450377. doi: 10.1142/S0217979224503776

[11] Yadav, P.K., & Verma, A.K. (2023). Analysis of the MHD flow of immiscible fluids with variable viscosity in an inclined channel. *Journal of Applied Mechanics and Technical Physics*, 64(4), 618−627. doi: 10.1134/S0021894423040077

[12] Yadav, S., Yadav, S., & Yadav, P.K. (2024). The mixed convection thermally radiated hybrid nanofluid flow through an inclined permeable shrinking plate with slip condition and inclined magnetic effect. *Chinese Journal of Physics*, 89, 1041-1050. doi: 10.1016/j.cjph.2023.12.039

[13] Yadav, P.K., & Yadav, N. (2023). A study on the flow of couple stress fluid in a porous curved channel. *Computers & Mathematics with Applications*, 152, 1−15. doi: 10.1016/j.camwa.2023.10.004

[14] Yadav, P.K., & Yadav, N. (2023). Entropy generation analysis in micropolar-couple stress fluid's flow in an inclined porous channel using Homotopy Analysis Method. *Chinese Journal of Physics*, 86, 469−496. doi: 10.1016/j.cjph.2023.10.024

[15] Yadav, P.K., & Verma, A.K. (2023). Analysis of the MHD flow of immiscible fluids with variable viscosity in an inclined channel. *Journal of Applied Mechanics and Technical Physics*, 64(4), 618−627. doi: 10.1134/s0021894423040077

[16] Kumar, A., & Yadav, P.K. (2023). Entropy generation analysis of non-miscible couple stress and Newtonian fluid in an inclined porous channel with variable flow properties: HAM Analysis. *International Journal of Modern Physics B*, 2450390. doi: 10.1142/s0217979224503909

[17] Kazakia, J.Y., & Rivlin, R.S. (1981). Run-up and spin-up in a viscoelastic fluid I. *Rheologica Acta*, 20, 111−127. doi: 10.1007/BF01513054

[18] Rivlin, R.S. (1982). Run-up and spin-up in a viscoelastic fluid. II. *Rheologica Acta*, 21, 107−111. doi: 10.1007/BF01736411

[19] Rivlin, R.S. (1982). Run-up and spin-up in a viscoelastic fluid. III. *Rheologica Acta*, 21, 213−222. doi: 10.1007/978-1-4612-2416-7_151

[20] Rivlin, R.S. (1983). Run-up and spin-up in a viscoelastic fluid. IV. *Rheologica Acta*, 22, 275−283. doi: 10.1007/BF01359127

[21] Narain, A., & Joseph, D.D. (1982). Linearized dynamics for step jumps of velocity and displacement of shearing flows of a simple fluid. *Rheologica Acta*, 21(3), 228−250. doi: 10.1007/BF01515712

[22] Devakar, M., & Iyengar, T.K.V. (2010). Run up flow of a couple stress fluid between parallel plates. *Nonlinear Analysis: Modelling and Control*, 15(1), 29−37. doi: 10.15388/na.2010.15.1.14362

[23] Devakar, M., & Iyengar, T.K.V. (2011). Run up flow of an incompressible micropolar fluid between parallel plates−A state space approach. *Applied Mathematical Modelling*, 35(4), 1751−1764. doi: 10.1016/j.apm.2010.10.007

[24] Qadri, S.Y., & Krishna, M.V. (2013). Run-Up Flow of a Maxwell Fluid through a Parallel Plate Channel. *American Journal of Computational Mathematics*, 3(2013), 109−120. doi: 10.4236/ajcm.2013.34039

[25] Krishna, M.V., & Qadri, S.Y. (2016). Run-up Flow of Oldroyd-B Fluid through a Parallel plate channel. *IOSR Journal of Mathematics*, 12(5), 1−8. doi: 10.9790/5728-1205030108

[26] Jibril, H.M., Jha, B.K., & Yusuf, K.L. (2019). Run-up Flow of an electrically Conducting Fluid In The Presence Of Transverse Magnetic Field in Annulus. *Mathematical Association of Nigeria*, 44, 98−107.

[27] Jha, B.K., Jibril, H.M., & Yusuf, K.L. (2023). Run-up flow of MHD fluid between parallel porous plates in the presence of transverse magnetic field. *Heat Transfer*, 52(3), 2651−2670. doi: 10.1002/htj.22799

[28] Honig, G., & Hirdes, U. (1984). A method for the numerical inversion of Laplace transforms. *Journal of Computational and Applied Mathematics*, 10(1), 113−132. doi: 10.1016/0377-0427(84)90075-X

[29] Rani, D., Mishra, V., & Cattani, C. (2018). Numerical inversion of Laplace transform based on Bernstein operational matrix. *Mathematical Methods in the Applied Sciences*, 41(18), 9231−9243. doi: 10.1002/mma.5188